analytical chemistry

Article

pubs.acs.org/ac

Dual Electrochemical and Physiological Apoptosis Assay Detection of in Vivo Generated Nickel Chloride Induced DNA Damage in *Caenorhabditis elegans*

Ian M. Huffnagle,[†,§] Alyssa Joyner,[‡,§] Blake Rumble,[†] Sherif Hysa,[†] David Rudel,*[,†] and Eli G. Hvastkovs*[,‡]

[†]Department of Biology, and [‡]Department of Chemistry, East Carolina University, Greenville, North Carolina 27858, United States

Supporting Information

ABSTRACT: Environmental nickel exposure is known to cause allergic reactions, respiratory illness, and may be responsible for some forms of cancer in humans. Nematodes are an excellent model organism to test for environmental toxins, as they are prevalent in many different environments. Nickel exposure has previously been shown to impact nematode life processes. In this study, *Caenorhabditis elegans* nematodes exposed to $NiCl_2$ featured high levels of programmed cell death (PCD) in a concentration-dependent manner as measured by counting apoptotic corpses in the nematode germ line. A green fluorescent protein (GFP) reporter transgene was used that highlights cell corpse engulfment by fluorescence microscopy. Analysis of the reporter in a *p53* mutant strain putatively indicates that the PCDs are a result of genomic DNA damage. In order to assay the potential genotoxic actions of $NiCl_2$, DNA was extracted from nematodes exposed to increasing concentrations of $NiCl_2$ and electrochemically assayed. In vivo damaged DNA was immobilized on pyrolytic graphite electrodes using the layer-by-layer (LbL) technique. Square-wave voltammograms were obtained in the presence of redox mediator, ruthenium trisbipyridine ($Ru(bpy)_3^{2+}$), that catalytically oxidizes guanines in DNA. Oxidative peak currents were shown to increase as a function of $NiCl_2$ exposure, which further suggests that the extracted DNA from nematodes exposed to the nickel was damaged. This report demonstrates that our electrochemical biosensor can detect damage at lower Ni concentrations than our physiological PCD assay and that the results are predictive of physiological responses at higher concentrations. Thus, a biological model for toxicity and animal disease can be assayed using an electrochemical approach.

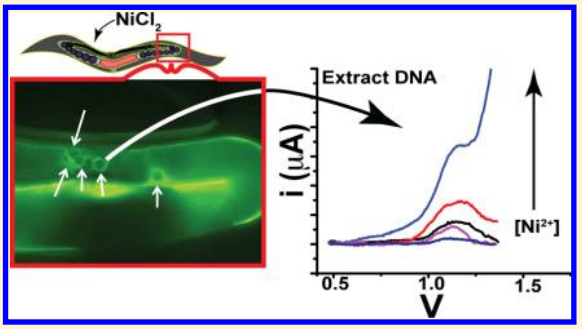

Nickel is a relatively common element used in a variety of industrial applications. Once mined or used, it can be released into the atmosphere where it can enter the groundwater and can eventually be consumed.[1] Human exposure to Ni-containing complexes comes primarily from drinking water, but inhalation and skin exposure are also possibilities.[1] Once ingested, Ni has been shown to be toxic and possibly carcinogenic.[2] Ni exposure has been linked to higher levels of nasal and lung cancers.[3−5] Ni toxicity can arise through glutathione depletion, but also via genotoxicity. Ni has been shown to be a moderate reactive oxygen species (ROS) promoter.[6] Additionally, Ni has been shown to enhance the toxicity of direct-acting genotoxins by impacting DNA packaging and repair processes by binding or effecting the expression of involved proteins.[7−10]

Environmental monitoring of Ni contamination has been performed using model organisms.[11,12] Nematodes are an excellent model as they are the most abundant multicellular animal, populate almost all environments, and are an integral part of almost every ecosystem. *Caenorhabditis elegans* and *Pristionchus pacificus* nematodes have been used to test the toxicity of Ni in different types of sediment.[13] Environmental levels of Ni were previously shown to impact the viability and resulting fecundity of these nematodes in a concentration-dependent manner. Ni complexes exhibited more toxicity, but water-soluble Ni^{2+} from $NiCl_2$ was shown to decrease nematode fecundity.[13] Fecundity decrease in nematodes exposed to soluble Ni^{2+} was intriguing in light of the genotoxic and epigenetic effects that Ni is known to cause. It was suggested that Ni exposure could cause genetic damage that led to the lower progeny rates. Therefore, it is necessary to monitor for possible genotoxicity caused by nickel exposure using complementary assays.

Counting cell deaths offers an in vivo assay to access physiological stresses on a cell, particularly those induced by toxins such as Ni.[14−16] Programmed cell death (PCD) or apoptosis is triggered so compromised cells do not hurt the organism as a whole. Once a cell has died, it is engulfed; an adjacent cell extends thin arms of its cell membrane around the cell corpse and takes it into the cytoplasm for delivery to a lysosome for degradation and recycling of molecules.[17,18]

Received: May 31, 2014
Accepted: July 21, 2014

dx.doi.org/10.1021/ac502007g | *Anal. Chem.* XXXX, XXX, XXX−XXX

Apoptosis is triggered by environmental, immune, and genomic stresses to the cell. The *p53* pathway monitors physical DNA damage in cells and instructs the cell to either fix the damage or to undergo PCD.[19]

Cell deaths in nematodes can be monitored by a number of microscopic mechanisms, for example, cell body morphology, apoptotic stains for cell corpses, and green fluorescent protein (GFP) transgenes that highlight cell corpses. Apoptosis can only be assayed in adult *C. elegans* in the germ line.[20] The 959 somatic cells of *C. elegans* are not replaced when damaged and not subjected to apoptosis. In contrast, germ cells constantly regenerate and differentiate into gametes and are carefully surveyed for quality to ensure a fit future generation. Thus, defective germ cells undergo apoptosis and die, which makes the nematode germ line ideal for toxicological studies.

Ni has been shown to induce apoptosis, but previous studies indicated that this may not be a response to DNA damage.[21] Thus, a second rapid and accurate assay that can monitor and/or confirm the potential of Ni to induce DNA damage as well as an assay that can look for damage at concentrations below what can be detected physiologically would greatly complement in vivo Ni toxicology studies.

Electrochemical techniques offer convenient, rapid, and inexpensive platforms for the analysis of DNA.[22−25] Electrochemical genotoxicity detection has been performed utilizing direct damaging genotoxins exposed to DNA immobilized on electrodes.[26−28] Layer-by-layer (LbL) modification has been effectively utilized to monitor DNA damage from a variety of substrates, and has the ability to produce rates of DNA damage from exposure over time,[26,29−32] while DNA hybridization sensors have been utilized to show that certain base sites can be specifically attacked by genotoxins.[33,34]

Herein, we demonstrate a dual strategy designed to elucidate the impact of $NiCl_2$ exposure to *C. elegans*. First, we exposed nematodes to higher concentrations of $NiCl_2$ to show that cell death does result from exposure to this xenobiotic. We also show that the PCDs are a response to DNA damage. Second, we employed an electrochemical biosensor to directly detect any in vivo DNA damage accumulated on genetic material extracted from the animal model. *C. elegans* were grown on media containing increasing concentrations of $NiCl_2$. DNA extracted from the nematode populations was immobilized on electrodes using a facile LbL strategy and electrochemically analyzed for damage. This report shows that DNA damage by Ni does induce apoptosis in nematodes and that a biochemical sensor can be utilized to assay for DNA damage at significantly lower Ni concentrations in comparison to the physiological assay. Thus, the damage detected by the sensor is predicative of programmed cell death at higher xenobiotic concentrations in an animal toxicology and disease model.

EXPERIMENTAL SECTION

Nematode Strains and Maintenance. *C. elegans* strains N2, MD701, KX84, and DJR1 were maintained at 20 °C on nematode growth media (NGM) seeded with *Escherechia coli* strain OP50.[35] N2 is the laboratory wild-type strain. MD701 (*bcls39v* [$P_{lim\text{-}7}$ *ced-1::gfp* and *lin 15*(+)]) contains a transgene that encodes for a membrane-bound GFP expressed in the *C. elegans* sheath cells. KX84 contains the same transgene as MD701 in a *ced-3*(*n2452*) homozygous loss-of-function mutant background. The DJR1 strain contains the same transgene as MD701 in a *cep-1*(*gk138*) homozygous deletion mutant background. Preparation of the different strains and synchronization of the nematode cultures is further explained in the Supporting Information.

Growth on $NiCl_2$. For extraction of DNA, mixed-staged N2 cultures were synchronized. L1 larvae were placed on 100 mm Petri dishes containing NGM agar with the indicated concentrations of $NiCl_2$. The $NiCl_2$ plates were seeded with antibiotic-killed and concentrated OP50. In brief, liquid OP50 cultures grown in Luria broth were started from a single isolated bacterial colony and grown overnight at 37 °C. Ampicillin and tetracycline were added to a final concentration of 20 and 10 mg L^{-1}, respectively. Cultures were allowed to sit overnight. Dead bacteria were pelleted and washed with PBS three times to remove the antibiotics. The final bacteria pellet was suspended and concentrated 30-fold in PBS. Bacterial cultures were streaked on NGM to ensure bacterial death. Using dead food aids in nematode growth and survival on higher $NiCl_2$ concentrations, a step necessary to obtain the number of animals required to extract DNA. For observation of cell deaths, mixed-staged MD701 cultures were synchronized. L1 larvae were then placed on live OP50-seeded NGM 100 mm plates containing the indicated concentrations of $NiCl_2$.

DNA Extraction. Animals were grown on seeded $NiCl_2$ NGM media for 6 days at 20 °C, i.e., two generations. DNA extractions were performed with relatively low $NiCl_2$ concentrations, 0, 5, 10, 25, and 50 μg L^{-1}, to be able to obtain enough material for an efficient DNA preparation. All steps other than those noted occur at 4 °C using ice-cooled buffers. Animals, eggs, and remaining bacteria were washed off the plates using PBS and placed in 15 mL conical tubes. Nematodes and eggs were pelleted and washed four times by suspension in PBS, centrifugation at 2000 rpm, and removal of the eluate. An amount of 2 mL of worm lysis buffer (20 mM Tris pH 7.5, 50 mM EDTA, 200 mM NaCl, 0.5% SDS, and 100 μg mL^{-1} proteinase K) was added to the nematode pellet, and the solution was then frozen in a −80 °C freezer overnight. The nematode suspension was next incubated at 55 °C with gentle agitation for 6 h. The solution was heated to 95 °C to heat-inactivate the proteinase K. Five units of DNase-free RNase A were added to the cooled suspension to degrade RNA, and the mixture was incubated at 37 °C for 4 h. A solution of a 1 part equilibrated phenol (pH 8)/1 part chloroform was freshly prepared. The aqueous DNA suspension was extracted four times with 5 mL of phenol/chloroform to remove residual proteins and carbohydrates contaminants. The DNA suspension was then extracted four times with 5 mL of chloroform to remove any residual phenol. The aqueous phase was removed and subdivided into microcentrifuge tubes. To each tube containing a set volume of the aqueous phase 1/20 volume of 5 M NaCl was added, and then the total volume was mixed with 2 vol of 100% ethanol to precipitate the DNA. The solution was left at −20 °C overnight. The DNA was pelleted at maximum speed in a microcentrifuge for 10 min. The eluate was removed, and the pellet was gently washed three times in 70% ethanol. Following removal of the last 70% ethanol wash, the pellet was allowed to air-dry until the edges became clear but the center was still slightly cloudy. The DNA was suspended in distilled water, and the concentration was determined using a nanodrop (Thermo). DNA quality was ensured by running a sample on an ethidium brodime stained agarose gel alongside 1kb DNA length standards.

Fluorescence Microscopy. Individual gonad arms were examined for GFP fluorescence using a Zeiss inverted Axiophot at 630× magnification. The cell corpses per gonad arm were

dx.doi.org/10.1021/ac502007g | *Anal. Chem.* XXXX, XXX, XXX−XXX

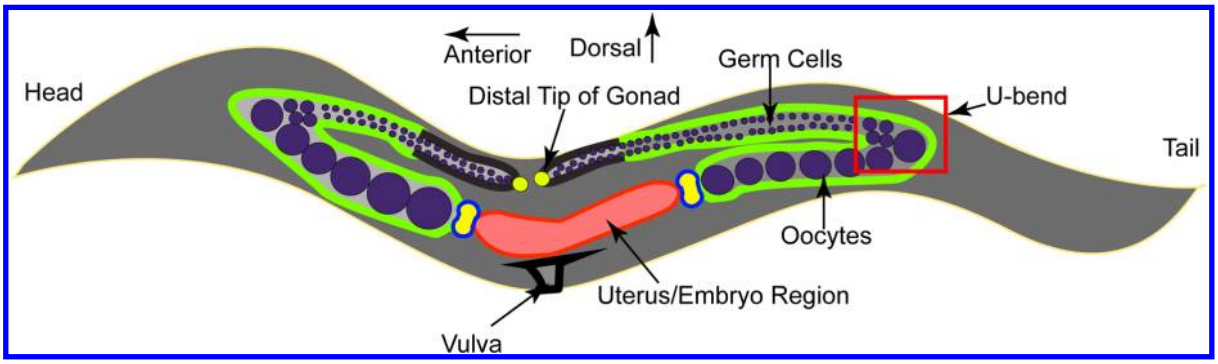

Figure 1. Simplified cartoon showing the nematode germcell region. Sheath cells surround germ cells and express GFP, which is represented by the green shown in the scheme.

counted. Fluorescent micrographs were taken using a Nikon DS-Fi2 camera and NIS-Elements Basic Research package version 4.0.

Electrochemical Assay Materials. Tris buffer was from Fluka, poly(diallyldimethylammonium chloride) (PDDA), poly(sodium 4-styrenesulfonate) (PSS), and tris(2,2′-bipyridyl)dichlororuthenium ($Ru(bpy)_3^{2+}$) were from Sigma, calf thymus DNA (sodium salt) was from Calbiochem. Purified 18 MΩ DI water was generated using a Siemens high-purity water system. All other chemicals for the electrochemical experiments were from Sigma and were reagent grade.

Electrode Preparation. Pyrolytic graphite (PG) electrodes (2 mm diameter) were abraded on grit SiC (Buehler) paper followed by rinsing and sonication in DI H_2O. After drying under an argon stream, the electrodes were then exposed to the following solutions: PDDA (50 μL droplet, 2 mg mL^{-1} in DI H_2O with 50 mM NaCl) for 15 min followed by PSS (3 mg mL^{-1} in DI H_2O with 50 mM NaCl). These steps were repeated twice. Then DNA (0.1 mg mL^{-1} in 10 mM Tris, 10 mM NaCl, pH 7.4) for 30 min was substituted for PSS in the following rounds of layering. The electrode was rinsed with DI water between each layer. The final film formation for the electrodes was $(PDDA/PSS)_2(PDDA/DNA)_2$.

Electrochemical Measurements. Layered DNA PG electrodes were placed in a standard three-electrode electrochemical cell (Pt counter, Ag/AgCl (saturated KCl) reference) in 10 mL buffer (50 mM ammonium acetate, pH 6.4) with 50 mM $Ru(bpy)_3^{2+}$. Square-wave voltammograms (SWV) were obtained using the following parameters: scan from 0 to +1.3 V, 15 Hz frequency, 4 mV step height, 25 mV amplitude. Raw SWV were analyzed using Origin 8.0 software and background-subtracted using the same SWV electrochemical response for a $(PDDA/PSS)_2$ electrode containing no DNA.

In Situ $NiCl_2$ DNA Damage Assay. Electrodes were formed using calf thymus DNA in the same manner as described above, but the DNA was at a concentration of 1.0 mg mL^{-1}. Electrodes were first oxidized in $Ru(bpy)_3^{2+}$ buffer solutions as described above to obtain the no damage background signal. The electrodes were then formed again and exposed to solutions of 8.0×10^3 $\mu g\ L^{-1}$ (150 μM) Ni^{2+}, 2 mM H_2O_2, or the combination of the two with and without 1 mM EDTA in 50 mM ammonium acetate buffer, pH 6.4, for 30 min at 37 °C. After incubation, the electrodes were rinsed with DI water and SWV were obtained in an identical fashion as described above.

Statistics. Statistical analysis was performed both using univariate analysis of variance with Tukey posthoc analysis in SPSS 19 and Excel for the MAC 2011, version 14.3.9.

RESULTS

Biological Data. As animals age their physiological processes within tissues change, for example, fertility, cell mitosis, and PCDs. Reproducible observation of cell corpses requires looking at the same tissues in animals of the same age. To do this, L1 animals were allowed to grow on $NiCl_2$ medium for 96 h. Thus, we looked at staged animals approximately 24 h into adulthood. Rather high concentrations of $NiCl_2$ were used for these studies, as the large numbers of animals required for a DNA preparation are not necessary. Additionally, as growth is retarded at higher $NiCl_2$ concentrations, animals were determined as adult based upon vulva morphology[36] and the presence of oocytes and embryos as well.[37] The hermaphrodite gonad consists of two rotationally symmetrical reflexed U-shaped tubes, each a complete ovo−testis, that both open into a common uterus at the anterior posterior of the animal.[37] A simplified cartoon showing this germcell region of the nematode is shown in Figure 1.

Cell death increases as a function of $NiCl_2$ exposure as assayed by imaging and counting germ cell corpses in the form of sheath cell engulfments. Sheath cells are very thin cells that form a tube around the developing germ line and engulf cell corpses on the dorsal side of the U-bend of the gonad, see box location in Figure 1. In the MD701, KX84, and DJR1 strains, the sheath cells express membrane bound GFP. When they engulf cells, the extending membrane forms a ring highlighting cell corpses (Figure 2a). We counted cell corpse engulfments in animals exposed to progressively higher concentrations of Ni. The average number of cell corpses counted per gonad arm increased in a statistically significant manner as $NiCl_2$ concentration increased (Figure 2c). White arrows in the figure indicate cell corpse engulfment. All $NiCl_2$ treatments of MD701 animals were statistically relevant compared to MD701 animals exposed to no $NiCl_2$ at a confidence interval of $p < 0.05$ for 400 $\mu g\ L^{-1}$ and $\ll 0.001$ for higher concentrations.

The apoptotic pathway is required for our assayed response to $NiCl_2$. Strain KX84 contains a mutation in the initiator caspase of the apoptotic pathway, CED-3/Caspase. In these animals apoptosis cannot occur, and thus, no cell corpses should be illuminated. In this background the glowing cell bodies we counted are not present (Figure 2b); thus we are counting PCDs. The response of KX84 for all $NiCl_2$ treatments

dx.doi.org/10.1021/ac502007g | Anal. Chem. XXXX, XXX, XXX−XXX

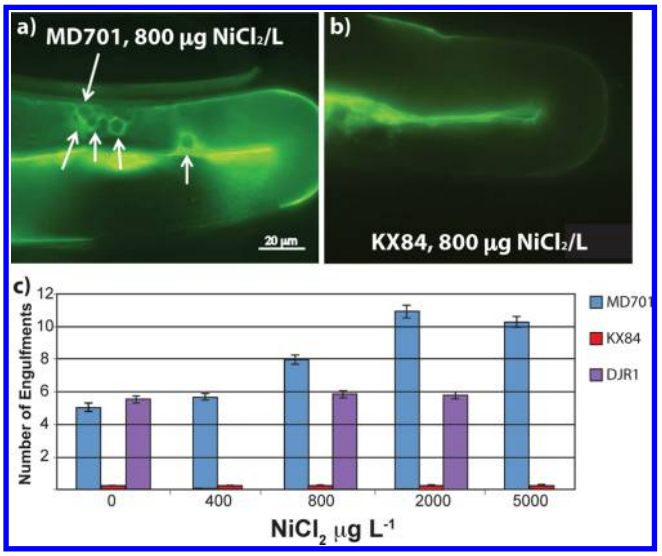

Figure 2. (a and b) Fluorescent micrographs of live adult hermaphrodites taken at the U-bends of representative gonad arms. Dorsal is toward the top; anterior toward the left. Animals were grown on 800 μg L^{-1} $NiCl_2$. (a) Strain MD701, a functionally wild-type animal with the exception of the expression of the *ced-1::gfp* transgene. MD701 shows increasing cell death correlated with $NiCl_2$ expression. White arrows indicate cell corpse engulfment. (b) Strain KX84 contains a deletion mutation in the initiator caspase of the apoptotic pathway; apoptosis should not occur and no cell corpses should be illuminated. (c) Average number of cell deaths as a function of $NiCl_2$ exposure with standard errors showing. Bar colors indicate *C. elegans* strain: blue, MD701; red, KX84; purple, DJR1. Numerical values are given in the table located in the Supporting Information.

compared to MD701 and DJR1 was significantly relevant at a confidence interval $p \ll 0.001$.

PCDs are a result of DNA damage. Strain DJR1 is homozygous mutant for a deletion allele in the *C. elegans cep-1* gene that encodes the nematode *p53* homologue. This strain does not make the *p53* protein that is responsible for triggering apoptosis in response to DNA damage. Animals with this genetic background did not show an increase in response to $NiCl_2$ beyond background levels (Figure 2c). The response of DJR1 compared to MD701 for 800 and 2000 μg L^{-1} was statistically relevant at a confidence interval $p \ll 0.001$.

Electrochemical Data. On the basis of the hypothesis that DNA damage is the reason for the cell death seen in Figure 2 micrographs, DNA was extracted from nematodes grown at much lower $NiCl_2$ exposure levels. The purpose for lower concentrations was to keep the nematodes viable and thus generate the populations necessary for DNA extraction and also demonstrate the sensitivity of the electrochemical assay compared to microscopy described above. Layer-by-layer DNA electrodes were generated following firmly established protocols.[26−29,31,38−40] The main difference between previously reported procedures and this report is the source of the genetic material. Typically, DNA from an animal source (e.g., calf thymus or salmon testes) is dissolved in buffer and immobilized on the electrode following the adsorption of a positively charged polymer or enzyme layer.[29] Anionic DNA readily adsorbs onto the cationic layers, and this process can be repeated to generate electrodes rich in DNA. DNA bases, primarily guanines, can be oxidized electrochemically,[22,41,42] and this electrochemical signal can be mediated via the addition of redox-active ruthenium trisbipyridine ($Ru(bpy)_3^{2+}$).[43−45] $Ru(bpy)_3^{2+}$ is oxidized at the electrode surface, and it can then oxidize guanine in the DNA films. This electrocatalytic cycle is shown below:

$$Ru(bpy)_3^{2+} \rightarrow Ru(bpy)_3^{3+} \quad \text{(at electrode)} \tag{1}$$

$$Ru(bpy)_3^{3+} + G(DNA) \rightarrow G^{\bullet+}(DNA) + Ru(bpy)_3^{2+} \tag{2}$$

The electrocatalytic reaction occurs kinetically faster when base pairing issues arise in the DNA helix.[29] For instance, DNA exposed to genotoxins, which can be attacked by nucleophilic sites on the guanine, results in slight base pairing alterations. This exposes the guanine to the $Ru(bpy)_3^{2+}$ and allows for closer approach of the ruthenium compound.[26,27] Upon oxidation, this results in higher electrochemical signals due to the faster cycling of re-reduced ruthenium at the electrode surface. Here, the DNA was damaged in vivo and harvested from the animal source itself.

Figure 3a shows background-subtracted SWV of layered DNA films where the DNA was extracted from *C. elegans* that

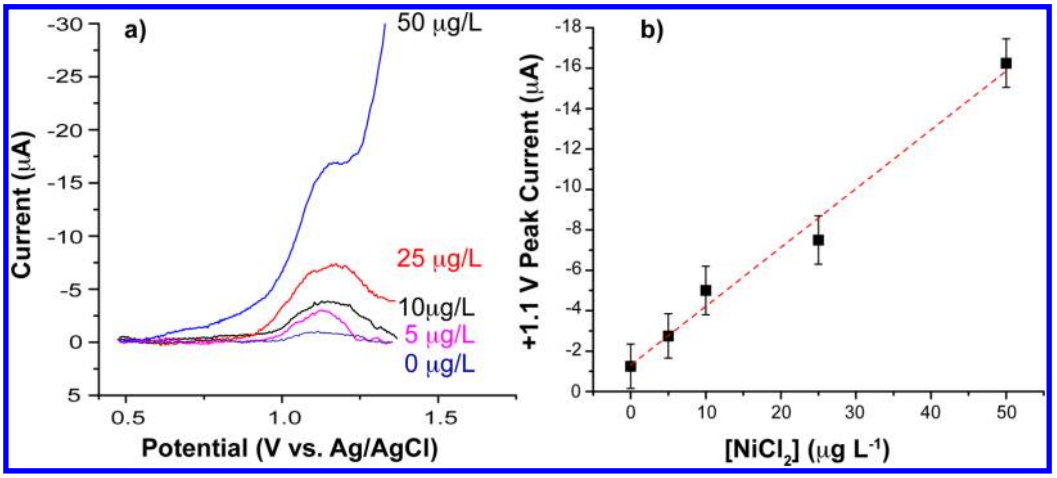

Figure 3. (a) Background-subtracted SWVs showing oxidation response from layered DNA electrodes in the presence of 50 μM $Ru(bpy)_3^{2+}$. DNA was extracted from nematode populations that had been exposed to the denoted concentration of Ni^{2+}. (b) Average peak current at ~+1.1 V vs Ag/AgCl as a function of $NiCl_2$ exposure concentration. Error bars show standard deviation for $n = 3$.

dx.doi.org/10.1021/ac502007g | *Anal. Chem.* XXXX, XXX, XXX−XXX

had been exposed to the denoted concentration of Ni^{2+}. Figure 3b shows that the peak current at approximately +1.1 V versus Ag/AgCl increases linearly as a function of the nickel exposure. The red dash in the figure shows the least-squares fit of the data and that the peak current increases in a linear fashion over the tested Ni^{2+} concentration range (R^2 = 0.98). A limit of detection based on 3:1 S/N was estimated at 0.22 μg L^{-1} Ni^{2+}, which is remarkably more sensitive than the biological assay described above. The lowest concentration of $NiCl_2$ tested for the physiological assay was 400 μg L^{-1} and gave a >95% confidence but required counting cell engulfments for more than 350 gonad arms (see Supporting Information Table S1). Lesser dosages with this range of counts did not yield a similarly significant result. This concentration is much higher than the top concentration of 50 μg L^{-1} $NiCl_2$ in which nematodes were grown for extraction of genomic DNA for the electrochemical assay.

Increases in peak current at this potential are consistent with a higher kinetic rate of $Ru(bpy)_3^{2+}$ oxidation at the electrode surface, which in turn is related to the structure of the DNA in the films. DNA that had been exposed to 50 μg L^{-1} Ni^{2+} showed much higher peak currents than DNA that was not exposed to Ni^{2+}. This suggests that exposure to nickel impacts the structure of the DNA in some manner that leads to easier access of solution-phase ruthenium primarily to oxidizable guanines, but adenines as well.[26]

Figure 4 shows DNA damage results using prefabricated LbL DNA electrodes. Here the DNA was from calf thymus and was

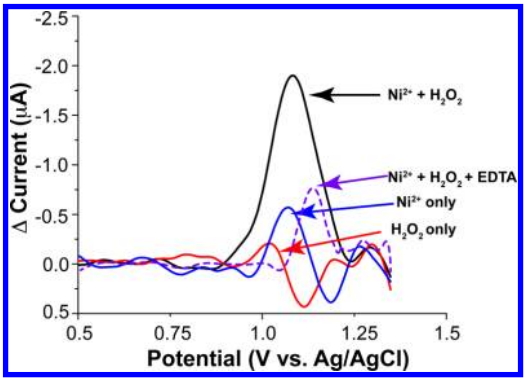

Figure 4. Background-subtracted SWV showing response of layered calf-thymus DNA electrodes in 50 μM $Ru(bpy)_3^{2+}$ after exposure to denoted xenobiotic solution. [Ni^{2+}] = 8 × 10^3 μg L^{-1} (150 μM), [H_2O_2] = 2 mM, [EDTA] = 1 mM, 50 mM ammonium acetate, pH 6.4.

placed on the electrode prior to any xenobiotic exposure. Higher concentrations of calf thymus DNA compared to nematode DNA as well as higher concentrations of xenobiotics Ni^{2+} and hydrogen peroxide were utilized in order to enhance the kinetics and facilitate the DNA damage process in a shorter (30 min) time frame. The plot shows background-corrected responses of LbL electrodes exposed to the denoted xenobiotic solution. Background correction here shows the difference between a DNA-modified electrode before and after exposure to the xenobiotic solution, i.e., the background is the response of the electrode not exposed to any xenobiotic. This corrects for any interelectrode signal deviations.[28,46] Exposure to $NiCl_2$ in the presence of hydrogen peroxide caused increases in the oxidation peak at ∼+1.1 V similar to what was seen from DNA extracted from the nematodes. Nickel is a moderate facilitator of reactive oxygen species and can undergo a Fenton reaction in the presence of H_2O_2 to produce them.[47] The data of Figure 4 are consistent with the oxidation or damage of DNA through the generation of ROS. The damaged DNA is then more accessible to the ruthenium compound, which results in the increasing oxidation peak potentials. DNA exposed to solutions containing only $NiCl_2$ or hydrogen peroxide, or the combination with 1 mM EDTA, did not show significant oxidation wave increases at this potential over the exposure period. EDTA sequesters the Ni^{2+} so that it cannot bind with DNA and react with H_2O_2, thus limiting the generation of ROS. Similar electrochemical responses have been seen using iron to generate ROS and DNA damage.[26]

DISCUSSION

The apoptosis assays indicate that cellular physiology in the *C. elegans* germ line is compromised upon nickel exposure (Figure 2). In the MD701 strain, higher concentrations of nickel exposure result in higher amounts of cell death. This strain is essentially a wild-type strain that expresses a *ced-1::gfp* fluorescent reporter so that its sheath cells can be imaged while engulfing cell corpses. Upon exposure to higher concentrations of $NiCl_2$, more cell corpses were observed being engulfed. Cell deaths occur to rid the germ line of damaged germ cells that may give rise to defective progeny. The engulfment process assayed in Figure 2 occurs in essence to rid the tissue of harmful dead and decaying cells and to recycle the cellular components for reuse by the nematode. Strain KX84 cannot initiate apoptosis at all; it does not express the initiator caspase CED-3. In this strain we should not observe cell deaths. The fact that the cell bodies we counted are no longer present in this strain indicates that we were counting cell corpses. Thus, strain KX84 provides a control for our apoptosis assay.

Strain DJR1 is homozygous for a mutation in *p53*. These animals cannot detect physical DNA damage. As a result, cells with a compromised genome are not identified and directed to die. DJR1 animals did not show increased cell deaths in response to $NiCl_2$. This implies that initiation of cell death requires the ability of the cell to look for damaged DNA. Thus, exposure to $NiCl_2$ must be damaging genomic DNA either directly or indirectly. Previous reports have monitored programmed cell deaths in response to Ni and found that cell deaths increased as a function of Ni concentration.[21] However, it also found that the *p53* DNA surveillance system was not required to initiate apoptosis. Several differences between previous reports and ours may have resulted in this discrepancy. Differences included time of Ni^{2+} exposure, concentration of Ni^{2+}, and differences in staining/imaging of the cell corpses. The difference between our results and the previous study emphasizes the necessity to look for actual DNA damage and to complement a physiological approach with an analytical technique that can assess DNA damage.

DNA was extracted from *C. elegans* nematodes that were exposed to a range of $NiCl_2$ concentrations. The concentrations used for the electrochemical DNA assay were much lower than the biological assay, which highlighted the sensitivity of the electrochemical detection. The lower $NiCl_2$ concentrations did not promote higher rates of cell engulfments like those seen in Figure 1. However, qualitatively, nematode cultures grow satisfactorily in $NiCl_2$ concentrations <25 μg L^{-1}, are noticeably slower growing at 25 μg L^{-1}, and nematodes are not healthy when grown on $NiCl_2$ concentrations >25 μg L^{-1}.

dx.doi.org/10.1021/ac502007g | *Anal. Chem.* XXXX, XXX, XXX–XXX

The extracted DNA was immobilized on electrodes in a LbL fashion. DNA extracted from nematodes that were exposed to $NiCl_2$ exhibited increased peak currents upon electrochemical oxidation in the presence of $Ru(bpy)_3^{2+}$. The peak currents increased linearly as a function of $NiCl_2$ concentration. Increases in peak current suggest higher amounts of damaged DNA in the samples that were exposed to higher concentrations of $NiCl_2$. More heavily damaged DNA allowed closer approach of $Ru(bpy)_3^{2+}$ primarily to oxidizable guanines, which enhances the redox kinetics and leads to higher peak currents

Genetic damage from nickel exposure can occur through a number of potential mechanisms.[1] One of these is the possibility that nickel undergoes Fenton-type reactions to produce reactive oxygen species that can attack and damage DNA.[47,48] For instance, Ni has been shown to produce reactive hydroxyl radicals in the presence of hydrogen peroxide that was formed enzymatically from superoxide. Hydroxyl radicals and other ROS can damage DNA, primarily guanines, in a number of ways, most notably through the formation of 8-oxo-guanine. Oxidized DNA has been detected electrochemically in a similar fashion utilizing similar transition metal redox-active species.[49]

Overall, the data of Figures 2 and 3 are consistent with $NiCl_2$ generating concentration-dependent DNA damage of some fashion in the nematodes. In an attempt to explain the origin of the damage leading to increases in peak current, an in situ assay was performed where preformed LbL DNA electrodes were exposed to Ni^{2+} and H_2O_2. The concentrations of DNA, Ni^{2+}, and H_2O_2 were higher in order to enhance the kinetics, as the in situ assay was performed in 30 min versus several days for the physiological assay. Data from Figure 4 show that nickel ions in the presence of hydrogen peroxide can produce higher oxidative peak currents in LbL DNA electrodes versus DNA electrodes that are not exposed to this combination. This is consistent with the formation of reactive oxygen species that damage the DNA, which leads to easier access of $Ru(bpy)_3^{2+}$ and higher peak currents upon oxidation. Exposure to only Ni^{2+} in the in situ assay did not produce significant peak current growth upon oxidation. Muted oxidation signals were also seen with the addition of EDTA to the assay, which demonstrates that the Ni^{2+} was involved in ROS production.

It is important to note that Figure 4 data presents only an isolated possibility and that ROS production alone is likely not the only possibility leading to the DNA damage detected in the physiological and electrochemical assays. Divalent metal ions including Ni^{2+} have been shown to bind to nucleases that affect DNA repair machinery such that damaged DNA bases cannot be properly excised from the nematode genome.[48] Additionally, exposure to nickel has been shown to down-regulate expression of proteins involved in DNA repair. Lastly, nickel has been shown to affect DNA packaging. All of these may lead to an increase in DNA damage from secondary xenobiotics and eventual ramifications that accompany the damage. In this fashion, the effects from direct damaging xenobiotics are putatively enhanced. In this particular study, however, *C. elegans* was not exposed to any added secondary xenobiotics. Therefore, any DNA damage that accumulated is either due to direct mutations caused by Ni, Ni-produced ROS, or other indirect Ni effects that make DNA more susceptible to damage, such as influencing repair and packaging processes. The genotoxic impact of additional xenobiotics in the presence of Ni^{2+} is an area of future focus.

CONCLUSIONS

Overall, we have demonstrated a relatively facile strategy utilizing an electrochemical sensor that can assay for in vivo generated DNA damage by directly monitoring the DNA extracted from an animal model. Biological data clearly showed that cell death results from exposure to $NiCl_2$ at higher concentrations. Cell death is most likely related to DNA damage. DNA extracted from *C. elegans* exposed to Ni^{2+} exhibited higher oxidative peak currents, and this peak current increase was shown to be dependent on $NiCl_2$ concentration. Thus, the electrochemical sensor and apoptosis assay complement each other. The apoptosis assay is able to determine dosages that result in physiological effects from likely DNA damage, while the electrochemical sensor can detect DNA damage at much lower nickel concentrations to enhance and confirm the results obtained in our apoptosis assay. Nematodes serve as a very important toxicology and disease model organism due to their ecological ubiquity, their properties that make them genetically, biochemically, and microscopically tractable, and their track-record for findings that translate into vertebrate, i.e., humans. Electrochemical sensors offer speed and cost benefits in the generation of biological information. Here, the electrochemical DNA damage sensor was utilized to measure genotoxicity generated in vivo.

ASSOCIATED CONTENT

Supporting Information

Additional experimental details and Table S1. This material is available free of charge via the Internet at http://pubs.acs.org.

AUTHOR INFORMATION

Corresponding Authors

*E-mail: rudeld@ecu.edu.

*E-mail: hvastkovse@ecu.edu.

Author Contributions

§I.M.H. and A.J. contributed equally to this work.

Notes

The authors declare no competing financial interest.

REFERENCES

(1) Cameron, K. S.; Buchner, V.; Tchounwou, P. B. *Rev. Environ. Health* **2011**, *26*, 81−92.

(2) Kasprzak, K. S.; Sunderman, F. W., Jr.; Salnikow, K. *Mutat. Res., Fundam. Mol. Mech. Mutagen.* **2003**, *533*, 67−97.

(3) Shen, H. M.; Zhang, Q. F. *Environ. Health Perspect.* **1994**, *102* (Suppl1), 275−282.

(4) Bruske-Hohlfeld, I. *Methods Mol. Biol.* **2009**, *472*, 3−23.

(5) Reger, R.; Morgan, W. *Occup. Med.* **1993**, *8*, 185−204.

(6) Murphy, J. T.; Bruinsma, J. J.; Schneider, D. L.; Collier, S.; Guthrie, J.; Chinwalla, A.; Robertson, J. D.; Mardis, E. R.; Kornfeld, K. *PLoS Genet.* **2011**, *7*, e1002013.

(7) Arita, A.; Munoz, A.; Chervona, Y.; Niu, J.; Qu, Q.; Zhao, N.; Ruan, Y.; Kiok, K.; Kluz, T.; Sun, H.; Clancy, H. A.; Shamy, M.; Costa, M. *Cancer Epidemiol., Biomarkers Prev.* **2013**, *22*, 261−269.

(8) Gadhia, S. R.; Calabro, A. R.; Barile, F. A. *Toxicol. Lett.* **2012**, *212*, 169−179.

(9) Tchou-Wong, K.; Kiok, K.; Tang, Z.; Kluz, T.; Arita, A.; Smith, P. R.; Brown, S.; Costa, M. *PLoS One* **2011**, *6*, e17728.

(10) Chervona, Y.; Arita, A.; Costa, M. *Metallomics* **2012**, *4*, 619−627.

(11) Besser, J. M.; Brumbaugh, W. G.; Kemble, N. E.; Ivey, C. D.; Kunz, J. L.; Ingersoll, C. G.; Rudel, D. *U. S. Geol. Surv., Sci. Invest. Rep.* **2011**, *2011−5225*, 53 plus appendices.

(12) Huguier, P.; Manier, N.; Meline, C.; Bauda, P.; Pandard, P. *Environ. Toxicol. Chem.* **2013**, *32*, 2100−2108.
(13) Rudel, D.; Douglas, C. D.; Huffnagle, I. M.; Besser, J. M.; Ingersoll, C. G. *PLoS One* **2013**, *8*, e77079.
(14) Yang, Y. X.; Li, X. L.; Wang, L.; Han, S. Y.; Zhang, Y. R.; Pratheeshkumar, P.; Wang, X.; Lu, J.; Yin, Y. Q.; Sun, L. J.; Budhraja, A.; Hitron, A. J.; Ding, S. Z. *Int. J. Oncol.* **2013**, *43*, 936−946.
(15) Ahamed, M.; Ali, D.; Alhadlaq, H. A.; Akhtar, M. J. *Chemosphere* **2013**, *93*, 2514−2522.
(16) Alarifi, S.; Ali, D.; Alakhtani, S.; Al Suhaibani, E. S.; Al-Qahtani, A. A. *Biol. Trace Elem. Res.* **2014**, *157*, 84−93.
(17) Conradt, B.; Xue, D. *WormBook* **2005**, 1−13.
(18) Mangahas, P. M.; Zhou, Z. *Semin. Cell Dev. Biol.* **2005**, *16*, 295−306.
(19) Gomez-Lazaro, M.; Fernandez-Gomez, F. J.; Jordan, J. *J. Physiol. Biochem.* **2004**, *60*, 287−307.
(20) Gartner, A.; Boag, P. R.; Blackwell, T. K. *WormBook* **2008**, 1−20.
(21) Cai, K.; Ren, C.; Yu, Z. *Toxicol. Ind. Health* **2010**, *26*, 249−256.
(22) Palecek, E. *Talanta* **2002**, *56*, 809−819.
(23) Palecek, E.; Jelen, F. *Crit. Rev. Anal. Chem.* **2002**, *32*, 261−270.
(24) Drummond, T. G.; Hill, M. G.; Barton, J. K. *Nat. Biotechnol.* **2003**, *21*, 1192−1199.
(25) Hvastkovs, E. G.; Buttry, D. A. *Analyst* **2010**, *135*, 1817−1829.
(26) Zhou, L.; Rusling, J. F. *Anal. Chem.* **2001**, *73*, 4780−4786.
(27) Mugweru, A.; Rusling, J. F. *Anal. Chem.* **2002**, *74*, 4044−4049.
(28) Yang, J.; Zhang, Z.; Rusling, J. F. *Electroanalysis* **2002**, *14*, 1494−1500.
(29) Rusling, J. F., Ed. *Biomolecular Films: Design, Function, and Applications*; Dekker: New York, 2003.
(30) Rusling, J. F.; Hvastkovs, E. G.; Hull, D. O.; Schenkman, J. B. *Chem. Commun.* **2008**, 141−154.
(31) Zhou, L.; Yang, J.; Estavillo, C.; Stuart, J. D.; Schenkman, J. B.; Rusling, J. F. *J. Am. Chem. Soc.* **2003**, *125*, 1431−1436.
(32) Hvastkovs, E. G.; Schenkman, J. B.; Rusling, J. F. *Annu. Rev. Anal. Chem.* **2012**, *5*, 79−105.
(33) Satterwhite, J. E.; Pugh, A. M.; Danell, A. S.; Hvastkovs, E. G. *Anal. Chem.* **2011**, *83*, 3327−3335.
(34) Satterwhite, J. E.; Trumbo, C. M.; Danell, A. S.; Hvastkovs, E. G. *Anal. Chem.* **2013**, *85*, 1183−1191.
(35) Brenner, S. *Genetics* **1974**, *77*, 71−94.
(36) Sternberg, P. W. *WormBook* **2005**, 1−28.
(37) Hubbard, E. J.; Greenstein, D. *WormBook* **2005**, 1−4.
(38) Diculescu, V. C.; Paquim, A. C.; Brett, A. M. O. *Sensors* **2005**, *5*, 377−393.
(39) Mbindyo, J.; Zhou, L.; Zhang, Z.; Stuart, J. D.; Rusling, J. F. *Anal. Chem.* **2000**, *72*, 2059−2065.
(40) Rusling, J. F. *Biosens. Bioelectron.* **2004**, *20*, 1022−1028.
(41) Palecek, E. *Electroanalysis* **1996**, *8*, 7−14.
(42) Palecek, E.; Fojta, M.; Tomschik, M.; Wang, J. *Biosens. Bioelectron.* **1998**, *13*, 621−628.
(43) Johnston, D. H.; Glasgow, K. C.; Thorp, H. H. *J. Am. Chem. Soc.* **1995**, *117*, 8933−8938.
(44) Johnston, D. H.; Thorp, H. H. *J. Phys. Chem.* **1996**, *100*, 13837−13843.
(45) Ontko, A. C.; Armistead, P. M.; Kircus, S. R.; Thorp, H. H. *Inorg. Chem.* **1999**, *38*, 1842−1846.
(46) Hvastkovs, E. G.; So, M.; Krishnan, S.; Bajrami, B.; Tarun, M.; Jansson, I.; Schenkman, J. B.; Rusling, J. F. *Anal. Chem.* **2007**, *79*, 1897−1906.
(47) Lloyd, D. R.; Phillips, D. H. *Mutat. Res., Fundam. Mol. Mech. Mutagen.* **1999**, *424*, 23−36.
(48) Beyersmann, D.; Hartwig, A. *Arch. Toxicol.* **2008**, *82*, 493−512.
(49) Dennany, L.; Forster, R. J.; White, B.; Smyth, M.; Rusling, J. F. *J. Am. Chem. Soc.* **2004**, *126*, 8835−8841.